CHALMERS
FINITE ELEMENT CENTER

PREPRINT 2003–22

Adaptive finite element methods for LES: Computation of the mean drag coefficient in a turbulent flow around a surface mounted cube using adaptive mesh refinement

Johan Hoffman

Chalmers Finite Element Center
CHALMERS UNIVERSITY OF TECHNOLOGY
Göteborg Sweden 2003

CHALMERS FINITE ELEMENT CENTER

Preprint 2003–22

Adaptive finite element methods for LES: Computation of the mean drag coefficient in a turbulent flow around a surface mounted cube using adaptive mesh refinement

Johan Hoffman

CHALMERS

Chalmers Finite Element Center
Chalmers University of Technology
SE–412 96 Göteborg Sweden
Göteborg, October 2003

Adaptive finite element methods for LES: Computation of the mean drag coefficient in a turbulent flow around a surface mounted cube using adaptive mesh refinement
Johan Hoffman
NO 2003–22
ISSN 1404–4382

Chalmers Finite Element Center
Chalmers University of Technology
SE–412 96 Göteborg
Sweden
Telephone: +46 (0)31 772 1000
Fax: +46 (0)31 772 3595
www.phi.chalmers.se

Printed in Sweden
Chalmers University of Technology
Göteborg, Sweden 2003

ADAPTIVE FEM FOR LES

JOHAN HOFFMAN

ABSTRACT. We consider the computation of the mean drag coefficient in a turbulent flow around a surface mounted cube using an adaptive finite element method, based on a posteriori error estimates, for a LES formulation of the problem. The a posteriori error estimates are based on the solution of an associated linearized dual problem that we approximate numerically. We prove a posteriori error estimates, and we present numerical examples using adaptive mesh refinement based on these a posteriori error estimates.

1. Introduction

In this paper we compute the mean drag coefficient in a *Large Eddy Simulation LES* of a turbulent flow around a surface mounted cube, using an adaptive finite element method based on *a posteriori error estimates* in terms of the solution of an associated linearized dual problem.

The idea of using duality arguments in a posteriori error estimation goes back to Babuška and Miller [2] in the context of postprocessing 'quantities of physial interest' in elliptic model problems. A framework for more general situations has since then been systematically developed by Eriksson & Johnson and Becker & Rannacher, with coworkers, see e.g. [10, 8, 3, 4, 26, 27]. For a more detailed account of the development of this framework, including references, we refer in particular to the review papers [8, 4]. For incompressible flow, applications of adaptive finite element methods based on this framework have been increasingly advanced with computation of functionals such as the drag force for 2d stationary benchmark problems in [3, 14], and drag and lift forces and pressure differences for 3d stationary benchmark problems in [19]. In [21], time dependent problems in 3d are considered, and the extension of this framework to LES is investigated in [18].

In LES, we apply a spatial averaging operator (filter) to the Navier-Stokes equations to obtain a new set of equations for the averaged (filtered) variables. Such an averaging process involves several mathematical issues that has to be addressed; such as a possible commutation error if the filter does not commute with differentiation, finding the correct boundary conditions for the filtered variables, and the problem of *closure* due to filtering of the non linear term in the Navier-Stokes equations. There is an extensive amount of work on LES, in particular regarding the closure problem and the construction of *subgrid*

Date: October 30, 2003.

Key words and phrases. adaptive finite element method, duality, a posteriori error estimate, turbulent viscous incompressible flow, large eddy simulation, surface mounted cube.

Johan Hoffman, Courant Institute of Mathematical Sciences, New York University, 251 Mercer Street, New York, NY 10012–1185, USA, *email*: hoffman@cims.nyu.edu.

models, and we refer to [13, 34] and the references therin for details. The commutation error is investigated in [7, 35], for example, and for work on boundary conditions (or near wall models) for LES we refer to [24, 32] and the references therin.

In [18], a posteriori error estimates in various norms and linear functionals of the filtered velocity field in a LES are presented. These estimates take into consideration both the numerical error from discretization of the filtered Navier-Stokes equations and the modeling error from unresolved subgrid scales, and are based on the solution of an associated linearized dual problem that contains information about error propagation in space-time. If we use a subgrid model in the computation, the subgrid modeling error is included in the a posteriori error estimates, which opens the possibility of comparing the error using different subgrid models. Altogether, the a posteriori error estimates open the possibility of adaptively choosing both an optimal mesh and an optimal subgrid model.

This approach to a posteriori error estimation with respect to the averaged solution, using duality teqniques, in terms of a modeling error and a discretization error was developed for convection-diffusion-reaction equations in [15, 22, 20, 16, 17]. Related approaches with a posteriori error estimates in terms of a modeling and a discretization contribution to the total error have been suggested. For example, more recently in [6] similar ideas are presented with applications to 2d convection-diffusion-reaction problems.

In this paper we consider the computation of the mean drag coefficient in a LES of a turbulent flow around a surface mounted cube, investigated experimentally in [30, 31] and computationally in e.g. [28], using an adaptive finite element method based on the teqniques developed in [18]. To the best knowledge of the author, this paper represents the first application of adaptive finite element methods, based on the solution of a dual problem, to the turbulent Navier-Stokes equations in 3d.

An outline of this paper is as follows: In Section 2 we present the Navier-Stokes equations as a model for viscous incompressible flow, and we state the discretization of the corresponding LES equations using the cG(1)cG(1) method. In Section 3 we prove a posteriori error estimates for the mean drag coefficient using the cG(1)cG(1) method, and we present a corresponding algorithm for adaptive mesh refinement, and in Section 4 we compute the mean drag coefficient using the teqniques developed in Section 3. We conclude with a summary and some remarks on future directions.

2. Turbulent flow and LES

The incompressible Navier-Stokes equations expressing conservation of momentum and incompressibility of a unit density constant temperature Newtonian fluid with constant kinematic viscosity $\nu > 0$ enclosed in a volume Ω in $\mathbb{R}^3$ with homogeneous Dirichlet boundary conditions, take the form: Find (u, p) such that

$$\begin{aligned} \dot{u} + (u \cdot \nabla)u - \nu\Delta u + \nabla p &= f && \text{in } \Omega \times I, \\ \nabla \cdot u &= 0 && \text{in } \Omega \times I, \\ u &= 0 && \text{on } \partial\Omega \times I, \\ u(\cdot, 0) &= u_0 && \text{in } \Omega, \end{aligned} \tag{2.1}$$

where $u(x,t) = (u_i(x,t))$ is the *velocity* vector and $p(x,t)$ the *pressure* of the fluid at (x,t), and f, u_0, $I = (0,T)$, is a given driving force, initial data and time interval, respectively. The quantity $\nu\Delta u - \nabla p$ represents the total fluid force, and may alternatively be expressed as

$$\nu\Delta u - \nabla p = \operatorname{div}\sigma(u,p), \tag{2.2}$$

where $\sigma(u,p) = (\sigma_{ij}(u,p))$ is the *stress tensor*, with components $\sigma_{ij}(u,p) = 2\nu\epsilon_{ij}(u) - p\delta_{ij}$, composed of the *stress deviatoric* $2\nu\epsilon_{ij}(u)$ with zero trace and an isotropic pressure: here $\epsilon_{ij}(u) = (u_{i,j}+u_{j,i})/2$ is the *strain tensor*, with $u_{i,j} = \partial u_i/\partial x_j$, and δ_{ij} is the usual Kronecker delta, the indices i and j ranging from 1 to 3. We assume that (2.1) is normalized so that the reference velocity and typical length scale are both equal to one. The Reynolds number Re is then equal to ν^{-1}.

2.1. **The averaged Navier-Stokes equations.** In a turbulent flow we are typically not able to resolve all scales of motion computationally. We may instead aim at computing a *running average* u^h of u on a scale h, defined by

$$u^h(x,t) = \frac{1}{h^3}\int_{Q_h} u(x+y,t)\; dy, \tag{2.3}$$

where $h = h(x,t)$ is a parameter related to the local resolution of the problem and $Q_h = \{y \in \mathbb{R}^3 : |y_i| \le h/2\}$. In the LES literature it is common to define the averaging operator through convolution by a certain filter function, and there is a multitude of filter functions being used. Though we only consider the case of the filter corresponding to (2.3) in this paper, the teqniques for a posteriori error estimation are general and apply to other filters, possibly with modifications for commutation errors associated with such filters.

By an extension of (u,p,u_0,f) to $\mathbb{R}^3$ by reflection for all $x \notin \overline{\Omega}$, the averaging operator (2.3) commutes with space and time differentiation. If we take the running average of the equations (2.1), corresponding to a LES, we obtain the following equations for u^h:

$$\begin{aligned} \dot{u}^h + (u^h\cdot\nabla)u^h - \nu\Delta u^h + \nabla p^h + F_h(u) &= f^h && \text{in } \Omega\times I,\\ \nabla\cdot u^h &= 0 && \text{in } \Omega\times I,\\ u^h &= 0 && \text{on } \partial\Omega\times I,\\ u^h(\cdot,0) &= u_0 && \text{in } \Omega, \end{aligned} \tag{2.4}$$

where we choose homogeneous Dirichlet boundary conditions for u^h, and $F_h(u) = \nabla\cdot\tau^h(u)$, where $\tau^h_{ij}(u) = (u_iu_j)^h - u_i^hu_j^h$ is the *Reynolds stress tensor*. The closure problem of LES is how to model $F_h(u)$ in terms of u^h in a subgrid model $\hat{F}_h(u^h)$, or $\tau^h(u)$ in a model $\hat{\tau}^h(u^h)$. In this paper we focus on the computation of chosen output functionals for the problem (2.4) using adaptive finite element methods, and we refer to [13, 34] and the references therin for work on subgrid modeling for LES.

A weak formulation of (2.4) reads: find $(u^h,p^h) \in L_2(I;[H_0^1(\Omega)]^3 \times L_2(\Omega))$, with $\dot{u}^h \in L_2(I;[L_2(\Omega)]^3)$ and $u^h(\cdot,0) = u_0^h$, such that

$$\begin{aligned} &(\dot{u}^h + u^h\cdot\nabla u^h, v) + (2\nu\epsilon(u^h),\epsilon(v)) - (p^h,\nabla\cdot v)\\ &-(\tau^h(u),\nabla v) + (\nabla\cdot u^h, q) = (f^h, v), \end{aligned} \tag{2.5}$$

for all $(v,q) \in L_2(I;[H_0^1(\Omega)]^3 \times L_2(\Omega))$, where we assume that $f^h \in L_2(I;[L_2(\Omega)]^3)$.

Here $L_2(\Omega)$ is the Hilbert space of Lebesgue square integrable functions on Ω, with scalar product $(\cdot,\cdot)$ and norm $\|\cdot\|$, and $H^s(\Omega)$ is the standard Hilbert space of functions in $L_2(\Omega)$ with also partial derivatives of order $\leq s$ in $L_2(\Omega)$. $H_w^s(\Omega)$ denotes the functions $v \in H^s(\Omega)$ that satisfies the Dirichlet boundary condition $v|_{\partial\Omega} = w$ (in the sense of traces), and in particular $H_0^s(\Omega)$ denotes the functions in $H^s(\Omega)$ that vanish on $\partial\Omega$. We let $\mathcal{C}(I;X)$ denote the space of all continuous functions $v : I \to X$ with $\max_{t\in I}\|v(t)\|_X < \infty$, where X denotes a Banach space with norm $\|\cdot\|_X$. For further details on the function spaces above we refer to [1, 11].

Assuming we have also Neumann boundary conditions, we denote Γ_D the part of the boundary $\partial\Omega$ where Dirichlet boundary conditions are specified, and $\Gamma_N = \partial\Omega \setminus \Gamma_D$ the part with Neumann boundary conditions. Now $H_w^s(\Omega)$ and $H_0^s(\Omega)$ denote the spaces of functions in $H^s(\Omega)$ that satisfies the Dirichlet boundary conditions on Γ_D.

The viscous term $(2\nu\epsilon(u^h),\epsilon(v))$ in the weak formulation (2.5) may alternatively be expressed as $(\nu\nabla u^h,\nabla v)$, where we have used that $(\epsilon(u^h),\nabla v) = (\epsilon(u^h),\epsilon(v))$ by the symmetry of the strain tensor. In the case of pure Dirichlet boundary conditions the two forms are equivalent, but in the case of Neumann boundary conditions on part of the boundary the difference is a boundary integral over Γ_N of the normal derivative of u multiplied by ν and the test function v.

2.2. **Discretization: the cG(1)cG(1) method.** The cG(1)cG(1) method is a variant of the G^2 method [25, 21, 18] using the continuous Galerkin method cG(1) in time instead of a discontinuous Galerkin method. With cG(1) in time the trial functions are continuous piecewise linear and the test functions piecewise constant. cG(1) in space corresponds to both test functions and trial functions being continuous piecewise linear. Let $0 = t_0 < t_1 < \ldots < t_N = T$ be a sequence of discrete time steps with associated time intervals $I_n = (t_{n-1}, t_n]$ of length $k_n = t_n - t_{n-1}$ and space-time slabs $S_n = \Omega \times I_n$, and let $W^n \subset H^1(\Omega)$ be a finite element space consisting of continuous piecewise linear functions on a mesh $\mathcal{T}_n = \{K\}$ of mesh size $h_n(x)$ with W_w^n the functions $v \in W^n$ satisfying the Dirichlet boundary condition $v|_{\Gamma_D} = w$.

We now seek functions (U_h, P_h), continuous piecewise linear in space and time, and the cG(1)cG(1) method for the averaged Navier-Stokes equations (2.4), with homogeneous Dirichlet boundary conditions and subgrid model $\hat{\tau}^h$, reads: For $n = 1, \ldots, N$, find $(U_h^n, P_h^n) \equiv (U_h(t_n), P_h(t_n))$ with $U_h^n \in V_0^n \equiv [W_0^n]^3$ and $P_h^n \in W^n$, such that

$$\begin{aligned}
&((U_h^n - U_h^{n-1})k_n^{-1} + \hat{U}_h^n \cdot \nabla \hat{U}_h^n, v) + (2\nu\epsilon(\hat{U}_h^n), \epsilon(v)) \\
&- (P_h^n, \nabla\cdot v) - (\hat{\tau}_n^h(\hat{U}_h^n), \nabla v) + (\nabla\cdot\hat{U}_h^n, q) \\
&+ \delta_1(\hat{U}_h^n\cdot\nabla\hat{U}_h^n + \nabla P_h^n, \hat{U}_h^n\cdot\nabla v + \nabla q) + \delta_2(\nabla\cdot\hat{U}_h^n, \nabla\cdot v) \\
&= (f^h, v + \delta_1(\hat{U}_h^n\cdot\nabla v + \nabla q)) \quad \forall (v,q) \in V_0^n \times W^n,
\end{aligned} \tag{2.6}$$

where $\hat{U}_h^n = \frac{1}{2}(U_h^n + U_h^{n-1})$, $\delta_1 = \frac{1}{2}(k_n^{-2} + |U|^2 h_n^{-2})^{-1/2}$ in the convection-dominated case $\nu < \hat{U}_h^n h_n$ and $\delta_1 = \kappa_1 h^2$ otherwise, $\delta_2 = \kappa_2 h$ if $\nu < \hat{U}_h^n h_n$ and $\delta_2 = \kappa_2 h^2$ otherwise, with

κ_1 and κ_2 positive constants of unit size, and

$$(v, w) = \sum_{K \in \mathcal{T}_n} \int_K v \cdot w \, dx,$$

$$(\epsilon(v), \epsilon(w)) = \sum_{i,j=1}^{3} (\epsilon_{ij}(v), \epsilon_{ij}(w)),$$

$$(\hat{\tau}^h(v), \nabla w) = \sum_{i,j=1}^{3} (\hat{\tau}_{ij}^h(v), \partial w_i / \partial x_j),$$

where we assume that the subgrid model $\hat{\tau}^h$ is sufficiently regular for the above integrals to make sense.

Again we note that the viscous term $(2\nu\epsilon(U_h), \epsilon(v))$ may alternatively occur in the form $(\nu\nabla U_h, \nabla v) = \sum_{i=1}^{3}(\nu\nabla(U_h)_i, \nabla v_i)$. In the case of Dirichlet boundary conditions the corresponding variational formulations are equivalent, but not so in the case of Neumann boundary conditions.

If we have a Neumann boundary conditions $\sigma \cdot n = g$ on $\Gamma_N \subset \partial\Omega$, then the right hand side of (2.6) is supplemented with an integral of $g \cdot v$ over Γ_N. This implements the Neumann boundary condition in weak form through the presence of a term $(-P_h, \nabla \cdot v) + (2\nu\epsilon(U_h), \epsilon(v)) = (\sigma, \epsilon(v))$ on the left hand side, which when integrated by parts generates an integral of $(\sigma \cdot n) \cdot v$ over Γ_N. If the viscous term appears in the form $(\nu\nabla U_h, \nabla v)$, the corresponding Neumann boundary condition has the form $\nu\nabla U_h \cdot n - P_h n = g$, where $\nabla U_h \cdot n$ is the derivative in the unit outward normal direction n. To simulate an outflow boundary condition we may use a Neumann boundary condition with $g = 0$ corresponding to a zero force at outflow, simulating outflow into a large empty reservoir. The alternative condition $\nu\nabla U_h \cdot n - P_h n = 0$ acts slightly differently as an approximation of a *transparent* outflow boundary condition, see [33].

2.3. **Computation of the mean drag force.** We want to compute an approximation of the quantity

$$N(\sigma(u^h, p^h)) = \frac{1}{|I|} \int_I \int_{\Gamma_0} \sum_{i,j=1}^{3} \sigma_{ij}(u^h, p^h) n_j \phi_i \; ds \; dt, \tag{2.7}$$

where (u^h, p^h) solves (2.4), ϕ is the trace on Γ_0 of a function in $H^1(\Omega)$, and $\Gamma_0 \subset \Gamma_D$ is a closed surface representing the boundary of a body immersed in the flow. If ϕ is a unit vector in the direction of the mean flow, (2.7) represents the mean of the drag force due to (u^h, p^h) on Γ_0 over a time interval I, and if ϕ is a unit vector in a direction perpendicular to the mean flow, (2.7) is the temporal mean of the lift force on Γ_0 due to (u^h, p^h) in that direction. With the idea of increasing the precision, see [14], we may use (2.4) and integration by parts to rewrite the surface integral in (2.7) as a volume integral, leading to the following expression for (2.7):

$$\begin{aligned} N(\sigma(u^h,p^h)) &= \frac{1}{|I|}\int_I (\dot{u}^h + u^h\cdot\nabla u^h - f^h,\varphi) - (p^h,\nabla\cdot\varphi) \\ &\quad +(2\nu\epsilon(u^h),\epsilon(\varphi)) - (\tau^h(u),\nabla\varphi) + (\nabla\cdot u^h,\theta)\ dt, \end{aligned} \tag{2.8}$$

for any $\varphi \in L_2(I;[H^1_{\phi,0}(\Omega)]^3)$, where $H^1_{\phi,0}(\Omega) = \{v \in H^1(\Omega) : v|_{\Gamma_0} = \phi, v|_{\Gamma_1} = 0\}$, $\Gamma_1 = \Gamma_D \setminus \Gamma_0$, and $\theta \in L_2(I;L_2(\Omega))$. We note that due to (2.4), this representation does neither depend on the choice of θ, nor the particular extension φ of ϕ being used. We are thus led to approximate $N(\sigma(u^h,p^h))$ by the quantity

$$\begin{aligned} N^h(\sigma(U_h,P_h)) &= \frac{1}{|I|}\int_I (\dot{U}_h + U_h\cdot\nabla U_h - f^h,\Phi) - (P_h,\nabla\cdot\Phi) \\ &\quad +(2\nu\epsilon(U_h),\epsilon(\Phi)) - (\hat{\tau}^h(U_h),\nabla\Phi) + (\nabla\cdot U_h,\Theta)\ dt, \end{aligned} \tag{2.9}$$

where $(U_h,P_h) \in L_2(I;V^n_0 \times W^n)$ and $(\Phi,\Theta) \in L_2(I;V^n_{\phi,0} \times W^n)$, with $V^n_{\phi,0} = \{v \in [W^n]^3 : v|_{\Gamma_0} = \phi, v|_{\Gamma_1} = 0\}$.

Remark 1. *Ultimately, we are of course interested in $N(\sigma(u,p))$ rather than $N(\sigma(u^h,p^h))$. The error $|N(\sigma(u,p)) - N(\sigma(u^h,p^h))|$ is typically of the order $\mathcal{O}(h)$, and in this paper we assume this error to be small compared to the error $|N(\sigma(u^h,p^h)) - N^h(\sigma(U_h,P_h))|$. For example, if we want to compute the mean drag force, so that $\phi = (1,0,0)$ in (2.7) with the positive x_1-direction being the mean flow direction, in the case of a rectangular box with upstream and downstream boundaries Γ_u and Γ_d respectively, corresponding unit outward normals $n_u = (-1,0,0)$ and $n_d = (1,0,0)$, and $n = (n_1,n_2,n_3)$ the unit outward normal of the whole box, we have*

$$\begin{aligned} &|N(\sigma(u,p)) - N(\sigma(u^h,p^h))| = |N(\sigma(u-u^h,p-p^h))| \\ &= |\frac{1}{|I|}\int_I\int_{\Gamma_0} (2\nu\epsilon_{11}(u-u^h) - (p-p^h))n_1\ ds\ dt| \equiv |I_u + I_p|, \end{aligned}$$

where

$$\begin{aligned} |I_p| = \quad & |\frac{1}{|I|}\int_I\int_{\Gamma_u} p(s) - p^h(s)\ ds - \int_{\Gamma_d} p(s) - p^h(s)\ ds\ dt| \\ = \quad & |\frac{1}{|I|}\int_I\int_{\Gamma_u} \frac{1}{h^3}\int_{Q_h} p(s) - p(s+y)\ dy\ ds - \int_{\Gamma_d}\frac{1}{h^3}\int_{Q_h} p(s) - p(s+y)\ dy\ ds\ dt| \\ = \quad & |\frac{1}{|I|}\int_I\int_{\Gamma_u} \frac{1}{h^3}\int_{Q_h} \nabla p(\xi_1)\cdot(-y)\ dy\ ds - \int_{\Gamma_d}\frac{1}{h^3}\int_{Q_h} \nabla p(\xi_2)\cdot(-y)\ dy\ ds\ dt| \\ & (\text{with } \xi_1,\xi_2 \in s+Q_h) \\ \leq \quad & 2\frac{1}{|I|}\int_I\int_{\Gamma_u\cup\Gamma_d} \max_{\xi\in s+Q_h} |\nabla p(\xi)|\ ds\ dt\ \frac{1}{h^3}\int_{Q_h}|y|\ dy \\ \leq \quad & 2\frac{1}{|I|}\int_I\int_{\Gamma_u\cup\Gamma_d} \max_{\xi\in s+Q_h} |\nabla p(\xi)|\ ds\ dt\ \frac{\sqrt{3}}{2}h \equiv Ch, \end{aligned}$$

and in a similar way we get that $|I_u| \leq \nu Ch$, where we have assumed sufficient regularity of (u,p) in the formal calculations above.

3. Adaptive finite element methods for LES

An adaptive algorithm includes feed-back from computation to achieve the computational goal with minimal computational cost. In an adaptive finite element method this feed-back from computation relies on a posteriori error estimates. In Algorithm 2, an adaptive algorithm for the computation of the mean drag force $N(\sigma(u^h,p^h))$ is presented, which is based on a posteriori error estimates of the form

$$|N(\sigma(u^h,p^h)) - N^h(\sigma(U_h,P_h))| \leq \sum_{K\in\mathcal{T}_n^k} \mathcal{E}_K^k, \tag{3.1}$$

where $\mathcal{E}_K^k$ is an *error indicator* for element K. We have here chosen the computational mesh $\mathcal{T}_n^k$ to be constant in time for each iteration k in the adaptive algorithm, and we have also chosen the time step length k_n to be constant in time, namely

$$k_n = \min_{K\in\mathcal{T}_n^k} \mathrm{diam}(K), \tag{3.2}$$

where $\mathrm{diam}(K)$ is the diameter of element K. A time dependent mesh could be used based on Theorem 5, but the possible gain must be compared to the increased computational cost of administrating a time dependent mesh. In this case, where we have chosen the mesh to be constant in time, the error indicators $\mathcal{E}_K^k$ contain the total contribution to the error from element K over the whole time interval I.

Algorithm 2 (Adaptive mesh refinement). *Start at $k = 0$, then do*

(1) *compute approximation to the primal problem (2.4) on $\mathcal{T}_n^k$*
(2) *compute approximation to the dual problem (3.3) on $\mathcal{T}_n^k$*
(3) *if $\sum_{K\in\mathcal{T}_k} \mathcal{E}_K^k < TOL$ then STOP, else*
(4) *refine a fixed fraction of the elements in $\mathcal{T}_n^k$ with largest $\mathcal{E}_K^k \to \mathcal{T}_n^{k+1}$*
(5) *set $k = k+1$, then goto (1)*

3.1. A posteriori error estimation.

Algorithm 2 is based on a posteriori error estimates of the form (3.1), which we derive by introducing the following linearized dual problem: Find $(\varphi,\theta) \in L_2(I;[H^2_{\psi_3}(\Omega)]^3 \times H^2(\Omega))$, with $(\dot\varphi,\dot\theta) \in \mathcal{C}(I;[H^1(\Omega)]^3 \times L_2(\Omega))$ and $\varphi(T) = 0$, such that

$$\begin{aligned} &\int_I -(v,\dot\varphi) + ((u^h\cdot\nabla)v + (v\cdot\nabla)U_h,\varphi) + (2\nu\epsilon(v),\epsilon(\varphi)) \\ &\quad -(q,\nabla\cdot\varphi) + (\nabla\cdot v,\theta)\ dt = \int_I (v,\psi_1) + (q,\psi_2)\ dt, \end{aligned} \tag{3.3}$$

for all $(v,q) \in L_2(I;[H^1_0(\Omega)]^3 \times L_2(\Omega))$ with $v(0) = 0$, given the data $\psi_1 \in L_2(I;[L_2(\Omega)]^3)$, $\psi_2 \in L_2(I;L_2(\Omega))$, and $\psi_3 \in L_2(I;[L_2(\partial\Omega)]^3)$, and where $(\nabla U_h\cdot\varphi)_j = (U_h)_{,j}\cdot\varphi$. We assume that there exists a unique solution to (3.3), and we note that for (3.3) to make sense we would only need that $(\varphi, \theta) \in L_2(I; [H^1_{\psi_3}(\Omega)]^3 \times L_2(\Omega))$ and $\dot{\varphi} \in L_2(I; [L_2(\Omega)]^3)$. The extra regularity is used for interpolation error estimates in the proof of Theorem 5.

The data ψ_i correspond to error estimates of different output functionals. For example, non zero ψ_1 and ψ_2 typically corresponds to point values or mean values of the velocity or the pressure respectively, see e.g. [19] for various examples of data corresponding to error estimates of different functionals. Here we want to compute the force on a body immersed in the fluid, and we are thus interested in computing an integral over the surface of this body. The corresponding data for the dual problem (3.3) is a non zero boundary condition ψ_3 on this surface $\Gamma_0 \subset \Gamma_D$. We introduce the following definitions:

$$
\begin{aligned}
&(v,w)_K = \int_K v \cdot w \; dx, \quad (v,w)_{\partial K} = \int_{\partial K} v \cdot w \; ds, \\
&\|v\|_K = (v,v)_K^{1/2}, \quad \|v\|_{\partial K} = (v,v)_{\partial K}^{1/2}, \\
&|v|_K = (\|v_1\|_K, \|v_2\|_K, \|v_3\|_K), \quad |v|_{\partial K} = (\|v_1\|_{\partial K}, \|v_2\|_{\partial K}, \|v_3\|_{\partial K}), \\
&|v|_{K,\infty} = (\max_{\eta \in I_n} \|v_1(\eta)\|_K, \max_{\eta \in I_n} \|v_2(\eta)\|_K, \max_{\eta \in I_n} \|v_3(\eta)\|_K), \\
&|v|_{\partial K,\infty} = (\max_{\eta \in I_n} \|v_1(\eta)\|_{\partial K}, \max_{\eta \in I_n} \|v_2(\eta)\|_{\partial K}, \max_{\eta \in I_n} \|v_3(\eta)\|_{\partial K}),
\end{aligned}
\tag{3.4}
$$

with the obvious simplifications for scalar functions v and w. To estimate interpolation errors over the space-time slabs $S_n = \Omega \times I_n$ in the proof of Theorem 5, we recall the following two lemmas from [18]:

Lemma 3. *For $(v,w) \in L_2(I_n; [L_2(\Omega)]^3 \times L_2(\Omega))$, $(\varphi, \theta) \in L_2(I_n; [H^2_0(\Omega)]^3 \times H^2(\Omega))$, with $(\dot{\varphi}, \dot{\theta}) \in \mathcal{C}(I_n; [L_2(\Omega)]^3 \times L_2(\Omega))$, and $(\Phi, \Theta) \in V_0^n \times W^n$ constant in time, we have*

$$
|\int_{I_n} (v, \varphi - \Phi) \; dt| \leq \int_{I_n} \sum_{K \in \mathcal{T}_n} |v|_K \cdot (C^k_{n,K} k_n |\dot{\varphi}|_{K,\infty} + C^h_{n,K} h^2_{n,K} |D^2 \varphi|_K) \; dt,
$$

$$
|\int_{I_n} (w, \theta - \Theta) \; dt| \leq \int_{I_n} \sum_{K \in \mathcal{T}_n} |w|_K (C^k_{n,K} k_n |\dot{\theta}|_{K,\infty} + C^h_{n,K} h^2_{n,K} |D^2 \theta|_K) \; dt,
$$

where $h_{n,K}$ is the diameter of element $K \in \mathcal{T}_n$, and D^2 measures second order derivatives with respect to x.

Lemma 4. *For $w \in L_2(I_n; [L_2(\Omega)]^3)$, $\varphi \in L_2(I_n; [H^2_0(\Omega)]^3)$, $\dot{\varphi} \in \mathcal{C}(I_n; [H^1(\Omega)]^3)$, and $\Phi \in V_0^n$ constant in time, we have*

$$
\begin{aligned}
&|\int_{I_n} \sum_{K \in \mathcal{T}_n} \int_{\partial K \setminus \partial \Omega} w \cdot (\varphi - \Phi) \; ds \; dt| \\
&\leq \int_{I_n} \sum_{K \in \mathcal{T}_n} |w|_{\partial K \setminus \partial \Omega} \cdot (C^k_{n,K} k_n |\dot{\varphi}|_{\partial K \setminus \partial \Omega, \infty} + C^h_{n,K} h^{3/2}_{n,k} |D^2 \varphi|_K) \; dt,
\end{aligned}
$$

where $h_{n,K}$ is the diameter of element $K \in \mathcal{T}_n$, and D^2 measures second order derivatives with respect to x.

In the rest of this paper we will refer to the *discretization error* as the error we get when approximating (2.5) by (2.6) assuming the subgrid model to be exact, and the *modeling error* as the error from the approximation $\hat{\tau}^h(U_h) \approx \tau^h(u)$ in (2.6). We note that for the discretization error we have a *Galerkin orthogonality property* (see e.g. [8]), which enables us to sharpen the a posteriori error estimates for this error. This is not the case for the modeling error, which may result in less sharp estimates for this error.

For simplicity, we present the a posteriori error estimate for the cG(1)cG(1) method with $\delta_1 = \delta_2 = 0$, which thus introduces an error in the a posteriori error estimates depending on the stabilization parameters δ_1 and δ_2. For the case $\delta_1, \delta_2 \neq 0$, we would adjust the dual problem (3.3) to be the transposition of the linearized variational form corresponding to the stabilized method, which is beyond the scope of this paper. In [23], the choices of different dual problems for stabilized finite element methods are investigated in the case of linear problems.

Theorem 5. *If u^h solves (2.4), (U_h, P_h) solves (2.6) with $\delta_1 = \delta_2 = 0$, and (φ, θ) solves (3.3) with data $\psi_1 = \psi_2 = \psi_3|_{\Gamma_1} = 0$ and $\psi_3|_{\Gamma_0} = \phi$, then*

$$|N(\sigma(u^h, p^h)) - N^h(\sigma(U_h, P_h))| \leq \sum_{K \in \mathcal{T}_n} \mathcal{E}_K = \sum_{K \in \mathcal{T}_n} (e_D^K + e_M^K) = e_D + e_M,$$

where e_D and e_M are the discretization and modeling errors respectively, defined by

$$\begin{aligned} e_D^K &= \frac{1}{|I|} \sum_{n=1}^N \int_{I_n} |R_1(U_h, P_h)|_K \cdot \omega_1 + |R_2(U_h)|_K \, \omega_2 + R_3(U_h) \cdot \omega_3 \; dt, \\ e_M^K &= \frac{1}{|I|} \sum_{n=1}^N \int_{I_n} |R_4(u, U_h)|_K \cdot \omega_4 + R_5(U_h) \cdot \omega_5 \; dt, \end{aligned}$$

with the residuals

$$\begin{aligned} R_1(U_h, P_h) &= \dot{U}_h + (U_h \cdot \nabla) U_h + \nabla P_h - \nu \Delta U_h + \nabla \cdot \hat{\tau}^h(U_h) - f^h, \\ R_2(U_h) &= \nabla \cdot U_h, \\ R_3(U_h) &= \frac{1}{2} \max_{S \subset \partial K} (|[(\nu \nabla U_h - \hat{\tau}^h(U_h))_1 \cdot n_S]|, ..., |[(\nu \nabla U_h - \hat{\tau}^h(U_h))_3 \cdot n_S]|), \\ R_4(u, U_h) &= \nabla \cdot (\tau^h(u) - \hat{\tau}^h(U_h)), \\ R_5(U_h) &= \frac{1}{2} \max_{S \subset \partial K} (|[(\hat{\tau}^h(U_h))_1 \cdot n_S]|, ..., |[(\hat{\tau}^h(U_h))_3 \cdot n_S]|), \end{aligned}$$

where $(M)_i$ denotes the i:th row of the matrix M and $[\cdot]$ denotes the jump over interior element boundaries $\partial K \setminus \partial\Omega$, and the dual weights

$$\begin{aligned}
\omega_1 &= C^k_{n,K} k_n |\dot\varphi|_{K,\infty} + C^h_{n,K} h^2_{n,K} |D^2\varphi|_K,\\
\omega_2 &= C^k_{n,K} k_n |\dot\theta|_{K,\infty} + C^h_{n,K} h^2_{n,K} |D^2\theta|_K,\\
\omega_3 &= C^k_{n,K} k_n |\dot\varphi|_{\partial K\setminus\partial\Omega,\infty} + C^h_{n,K} h^{3/2}_{n,k} |D^2\varphi|_K,\\
\omega_4 &= |\varphi|_K,\\
\omega_5 &= |\varphi|_{\partial K\setminus\partial\Omega,\infty},
\end{aligned}$$

where $h_{n,K}$ is the diameter of element $K \in \mathcal{T}_n$, D^2 measures second order derivatives with respect to x, and $C^h_{n,K}, C^k_{n,K}$ represent interpolation constants.

Proof. To derive a posteriori error estimates for $N(\sigma(u^h,p^h))$, the natural quantity to consider is the difference between (2.8) and (2.9), see [14, 19]. If we set $(\varphi,\theta) = (\Phi,\Theta) \in L_2(I; V^n_{\phi,0} \times W^n)$ in (2.8) and then subtract (2.9), we get

$$\begin{aligned}
&N(\sigma(u^h,p^h)) - N^h(\sigma(U_h,P_h)) \qquad (3.5)\\
= \;& \frac{1}{|I|}\int_I (\dot u^h + u^h\cdot\nabla u^h, \Phi) - (p^h, \nabla\cdot\Phi) + (2\nu\epsilon(u^h), \epsilon(\Phi)) - (\tau^h(u), \nabla\Phi) + (\nabla\cdot u^h, \Theta)\\
&-((\dot U_h + U_h\cdot\nabla U_h, \Phi) - (P_h, \nabla\cdot\Phi) + (2\nu\epsilon(U_h), \epsilon(\Phi)) - (\hat\tau^h(U_h, \nabla\Phi) + (\nabla\cdot U_h, \Theta))\; dt.
\end{aligned}$$

The dual problem (3.3) with data

$$\psi_1 = \psi_2 = \psi_3|_{\Gamma_1} = 0, \quad \psi_3|_{\Gamma_0} = \phi, \tag{3.6}$$

and ϕ from (2.7), gives that

$$\begin{aligned}
& \frac{1}{|I|}\int_I (\dot u^h + u^h\cdot\nabla u^h, \varphi) - (p^h, \nabla\cdot\varphi) + (2\nu\epsilon(u^h), \epsilon(\varphi)) - (\tau^h(u), \nabla\varphi) + (\nabla\cdot u^h, \theta)\\
&-((\dot U_h + U_h\cdot\nabla U_h, \varphi) - (P_h, \nabla\cdot\varphi) + (2\nu\epsilon(U_h), \epsilon(\varphi)) - (\hat\tau^h(U_h), \nabla\varphi) + (\nabla\cdot U_h, \theta)\; dt\\
= \;& \frac{1}{|I|}\int_I -(\dot\varphi, e) + (u^h\cdot\nabla e + e\cdot\nabla U_h, \varphi) - (p^h - P_h, \nabla\cdot\varphi) + (2\nu\epsilon(e), \epsilon(\varphi))\\
&+(\nabla\cdot e, \theta) + (\hat\tau^h(U_h) - \tau^h(u), \nabla\varphi)\; dt = \frac{1}{|I|}\int_I (\hat\tau^h(U_h) - \tau^h(u), \nabla\varphi)\; dt, \qquad (3.7)
\end{aligned}$$

using partial integration with $\varphi(T) = e(0) = 0$, where $e = u^h - U_h$, and that $(u^h\cdot\nabla)u^h - (U_h\cdot\nabla)U_h = (u^h\cdot\nabla)e + (e\cdot\nabla)U_h$. By (2.5), (3.5), and (3.7), we then have that

$$\begin{aligned}
&N(\sigma(u^h,p^h)) - N^h(\sigma(U_h,P_h))\\
= \;& \frac{1}{|I|}\int_I ((\dot U_h + U_h\cdot\nabla)U_h - f^h, \varphi - \Phi) - (P_h, \nabla\cdot(\varphi - \Phi)) + (\nabla\cdot U_h, \theta - \Theta)\\
&+(2\nu\epsilon(U_h) - \hat\tau^h(U_h), \nabla(\varphi - \Phi)) + (\hat\tau^h(U_h) - \tau^h(u), \nabla\varphi)\; dt. \qquad (3.8)
\end{aligned}$$

From this *error representation formula* there are various possibilities to estimate the integrals in (3.8).

Integration by parts in the viscous term results in non zero boundary integrals over interior element boundaries $\partial K \setminus \partial\Omega$, for each t, since ∇U is piecewise constant in x over the elements and thus discontinuous over interior element boundaries, and we have the same problem for the subgrid model $\hat{\tau}^h(U_h)$. This is not the case for the pressure term since the pressure is continuous in x over element boundaries, and so is $\varphi - \Phi$ and $\tau^h(u)$.

To estimate these element boundary integrals we use a standard finite element teqnique, see e.g. [9], where we first rewrite the sum of interior element boundary integrals as a sum of jumps in normal derivative of the form $[\nu\nabla U_h \cdot n_S]$ over all interior faces S in $\mathcal{T}_n$, with n_S being a globally defined unit normal vector associated with the face S. We then attribute half of the jump to each of the two elements sharing the face and rewrite the sum again over the elements $K \in \mathcal{T}_n$, to get

$$
\begin{aligned}
&|N(\sigma(u^h,p^h)) - N^h(\sigma(U_h,P_h))| \\
&\leq \frac{1}{|I|}\sum_{n=1}^{N}\int_I \{\, |(\dot{U}_h + (U_h\cdot\nabla)U_h + \nabla P_h - \nu\Delta U_h + \nabla\cdot\hat{\tau}^h(U_h) - f^h, \varphi - \Phi)| \\
&+ |(\nabla\cdot U_h, \theta - \Theta)| + |\sum_{K\in\mathcal{T}_n}\int_{\partial K\setminus\partial\Omega}\frac{1}{2}[(\nu\nabla U_h - \hat{\tau}^h(U_h))\cdot n_S]\cdot(\varphi - \Phi)\; ds| \\
&+ |(\nabla\cdot(\tau^h(u) - \hat{\tau}^h(U_h)), \varphi)| + |\sum_{K\in\mathcal{T}_n}\int_{\partial K\setminus\partial\Omega}\frac{1}{2}[\hat{\tau}^h(U_h)\cdot n_S]\cdot\varphi\; ds|\;\}\; dt.
\end{aligned}
$$

We finally use Cauchy-Schwarz inequality for each element, and then Lemma 3 and Lemma 4 to estimate the interpolation errors.

□

Remark 6. *The modification of Theorem 5 for the case of inhomogeneous Dirichlet boundary conditions on part of the boundary, such as a given inflow velocity, is straight forward by incorporating this boundary condition in the corresponding trial spaces.*

3.2. **Remarks on the linearization error in the dual problem.** The a posteriori error estimate in Theorem 5 is designed to be useful in an adaptive algorithm as a stopping criterion, a refinement criterion for the space and time discretization, and an error indicator for the subgrid model. To evaluate the error bounds in Theorem 5 we approximate the dual weights ω_i numerically, by computing approximate solutions to the dual problem (3.3). In this paper we solve the dual problem using the cG(1)cG(1) method on the same computational mesh as we use for the primal problem, which is neither necessary nor optimal but is chosen here for reasons of simplicity. In the computation of the dual problem we do not have access to u^h, the solution of (2.4). Instead we approximate u^h by U_h, a finite element approximation of u^h, which thus introduces a linearization error $u^h - U_h$ in the dual problem.

Here we make the assumption that U_h converges to u^h pointwise and that thus the linearization error converges pointwise to zero. Such an assumption gives some justification for using Theorem 5, although there may still be problems when the computational mesh is not fine enough, and/or the subgrid model is not accurate enough. Practical experience from using this type of a posteriori error estimates for adaptive mesh refinement for various problems has been positive, with effective mesh refinement criterions and sharp a posteriori error estimates, see e.g. [19, 4] for examples of incompressible flow.

Alternative forms of the linearized dual problem (3.3) are possible. For example, one may linearize the dual problem at u, the exact solution of (2.1). Although, this is not practical for numerical approximation of the dual problem since the corresponding linearization error $u - U_h$ can never be pointwise small in a LES. Typically the error $u - U_h$ is large pointwise, since u contains finer scales than U_h.

4. Numerical results

We now use Algorithm 2 to compute the mean drag coefficient for a surface mounted cube in a turbulent channel flow. We use the cG(1)cG(1) method for both the primal and the dual problem, on tetrahedral meshes $\mathcal{T}_n^k$. In the definition of the averaging operator (2.3) corresponding to the LES for the adaptive step k, we let $h = h(x)$ be defined to be the piecewise constant function that equals the diameters of the tetrahedrons in $\mathcal{T}_n^k$.

We use no subgrid model in the computations, but we use the following scale similarity subgrid model from [29] to estimate the size of the modeling residual $R_4(u, U_h) = \nabla \cdot \tau^h(u)$:

$$\tau_{ij}^h(u) \approx C_L \tau_{ij}^{2h}(u^h) = C_L((u_i^h u_j^h)^{2h} - (u_i^h)^{2h}(u_j^h)^{2h}), \tag{4.1}$$

with $C_L = 1$, and u^h approximated by U_h in the computations.

4.1. Flow around a surface mounted cube.

We consider the problem of a turbulent flow around a surface mounted cube, investigated in [30, 31, 28]. In our computational model we use the Navier-Stokes equations to model the incompressible fluid around a cubic body of dimension $H \times H \times H$ that sits on the floor of a rectangular channel of length $15H$, height $2H$, and width $7H$, centered at $(3.5H, 0.5H, 3.5H)$. At the inlet we use a velocity profile interpolated from experiments, we use no slip boundary conditions on the body and the vertical boundaries, slip boundary conditions on the lateral boundaries, and a transparent outflow boundary condition. The viscosity ν is chosen to give a Reynolds number $Re = U_b H/\nu = 40.000$, where we have used $U_b = 1.0$.

4.2. Adaptive computation of the mean drag coefficient.

In Figure 1 we show a snapshot of the solution and the corresponding computational mesh after 13 adaptive mesh refinements, using Algorithm 2 to compute an approximation of the mean drag coefficient $\bar{c}_D$ over a time interval $I = [T_0, T]$, with $T_0 = 10$ and $T = 20$, defined by

$$\bar{c}_D = \frac{1}{|T - T_0|} \int_{T_0}^{T} c_D(t)\ dt, \tag{4.2}$$

where $c_D(t)$ is the drag coefficient at time t, and $\bar{c}_D = N(\sigma(u^h, p^h)) \times 2/(H^2 U_b^2)$. To estimate the computational cost of computing an approximation of $\bar{c}_D$ we study the solution of the corresponding dual problem with data according to (3.6), and $\phi = (2/(H^2 U_b^2), 0, 0)$ on the surface of the cube. One way to estimate the computational cost is through the

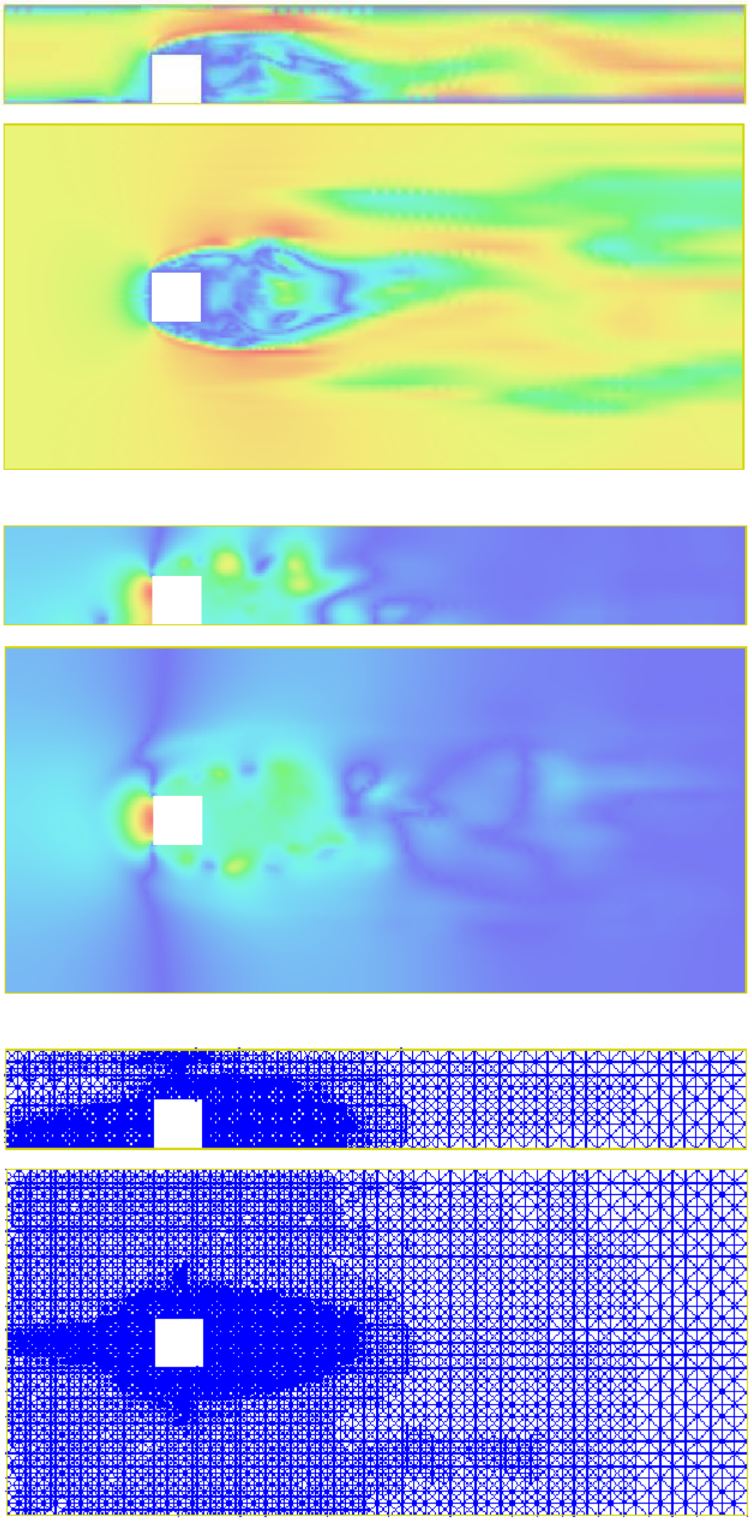

FIGURE 1. Primal velocity $|u|$ (upper), primal pressure $|p|$ (middle), and computational mesh (lower), after 13 adaptive mesh refinements at $z = 3.5H$ and $y = 0.5H$.

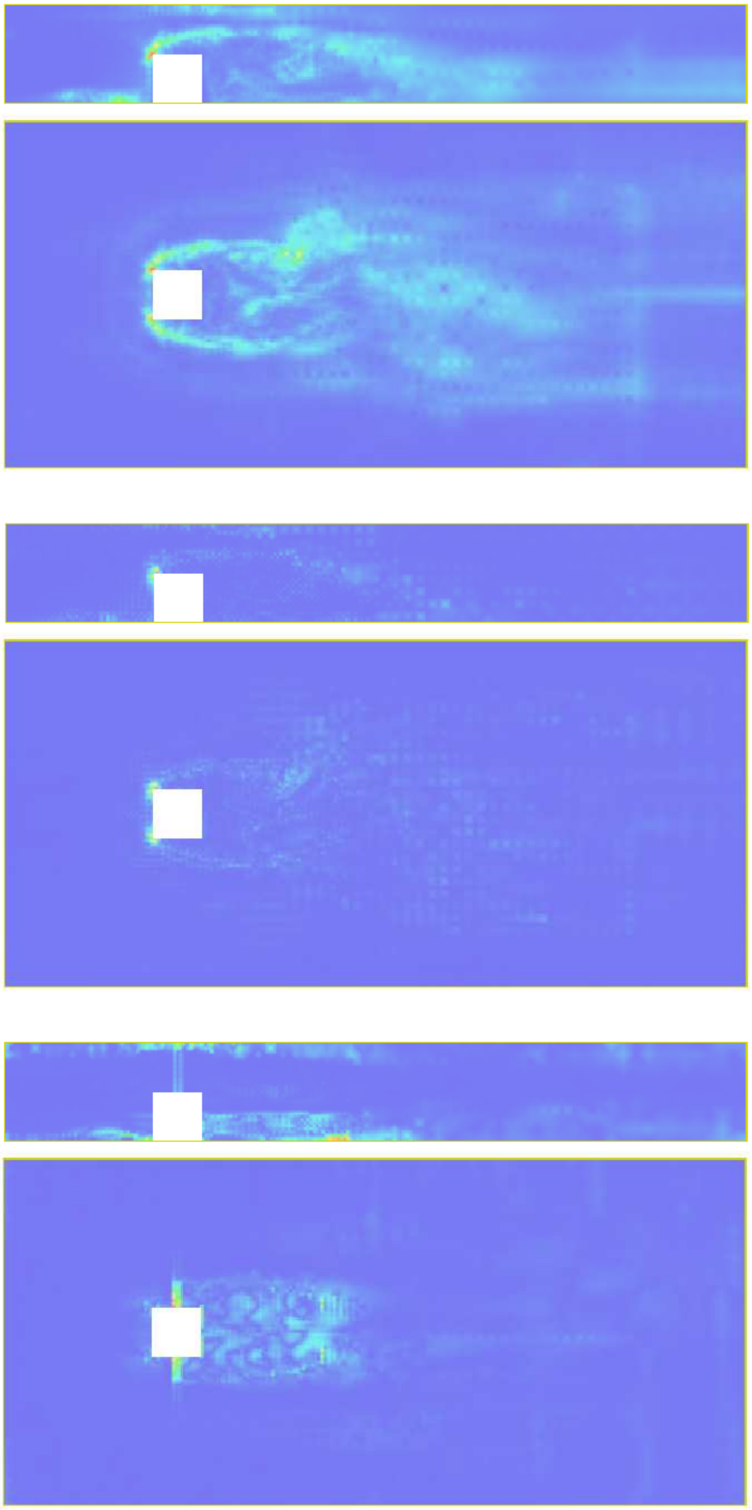

FIGURE 2. Residuals $|R_1(U_h, P_h)|$ (upper), $|R_2(U_h)|$ (middle), and $|R_4(u, U_h)|$ (lower), after 13 adaptive mesh refinements at $z = 3.5H$ and $y = 0.5H$.

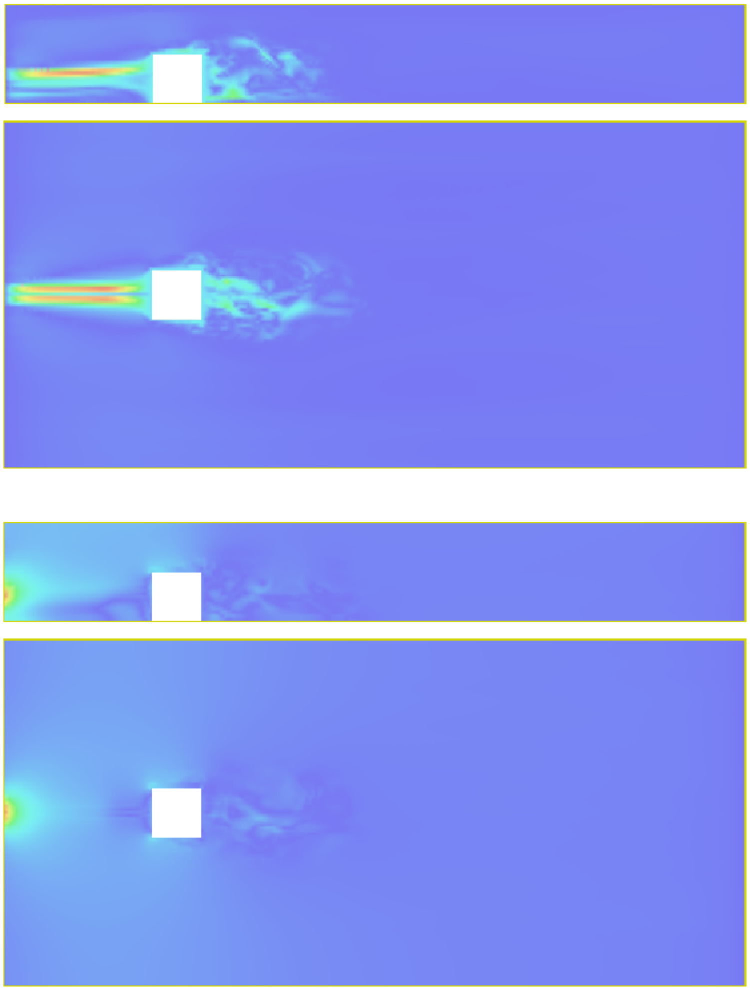

FIGURE 3. Dual velocity $|\varphi|$ (upper) and dual pressure $|\theta|$ (lower), after 13 adaptive mesh refinements at $z = 3.5H$ (upper) and $y = 0.5H$ (lower).

computation of *stability factors*, see e.g. [19]. For example, in Figure 5 we plot the stability factor $S_{1,1}(T_0)$, defined by

$$S_{1,1}(T_0) = \frac{1}{|T - T_0|} \int_{T_0}^{T} \int_{\Omega} |\varphi(x,t)| \; dx \; dt, \tag{4.3}$$

where φ is the solution of the dual problem (3.3) with data as above. We find that the computational cost at first increases with the length of the time interval $[T_0, T]$ (T fix, T_0 varying), but when the interval exceeds a certain length the computational cost does not increase significantly beyond a certain level. Thus the computational cost of computing $\bar{c}_D$ is relatively constant for time intervals longer than a certain length in this problem.

The error indicator $\mathcal{E}_K^k$ in Algorithm 2, giving the computational mesh in Figure 1, depends on the product of the residuals and the dual solution. In Figure 2 we show a

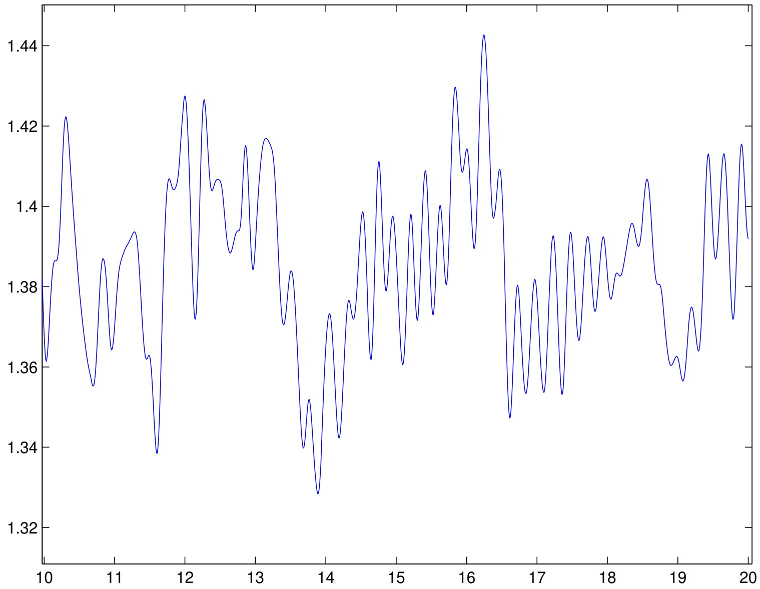

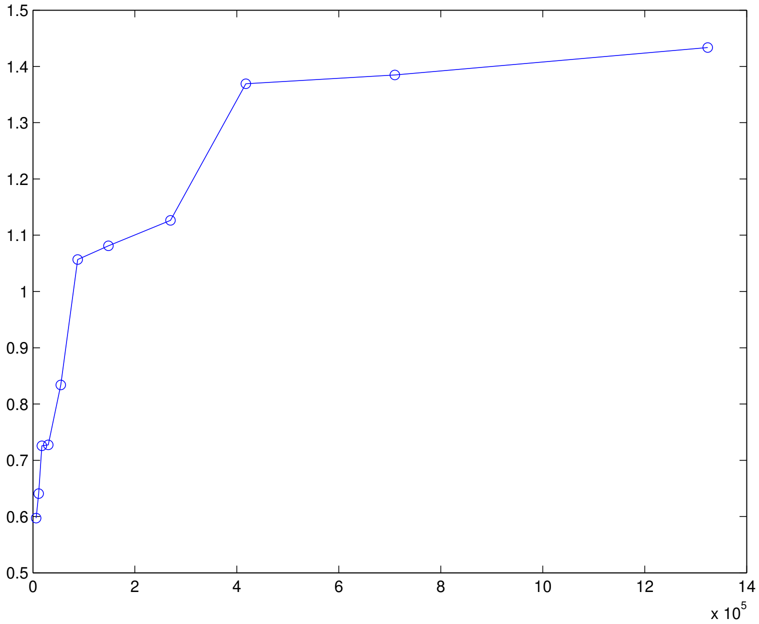

FIGURE 4. Drag coefficient $\bar{c}_D$ as a function of time, after 13 adaptive mesh refinements (upper), and mean drag coefficient $\bar{c}_D$ over the time interval $[10, 20]$, as a function of the number of degrees of freedom (lower).

snapshot of the residuals after 13 adaptive mesh refinements, and in Figure 3 we show a snapshot of the corresponding dual solution.

We find that the discretization residuals $R_1(U_h, P_h)$, corresponding to the momentum equation, and $R_2(U_h)$, corresponding to the continuity equation, are large at the upstream corners of the cube and along the high velocity streaks around the cube, and the modeling

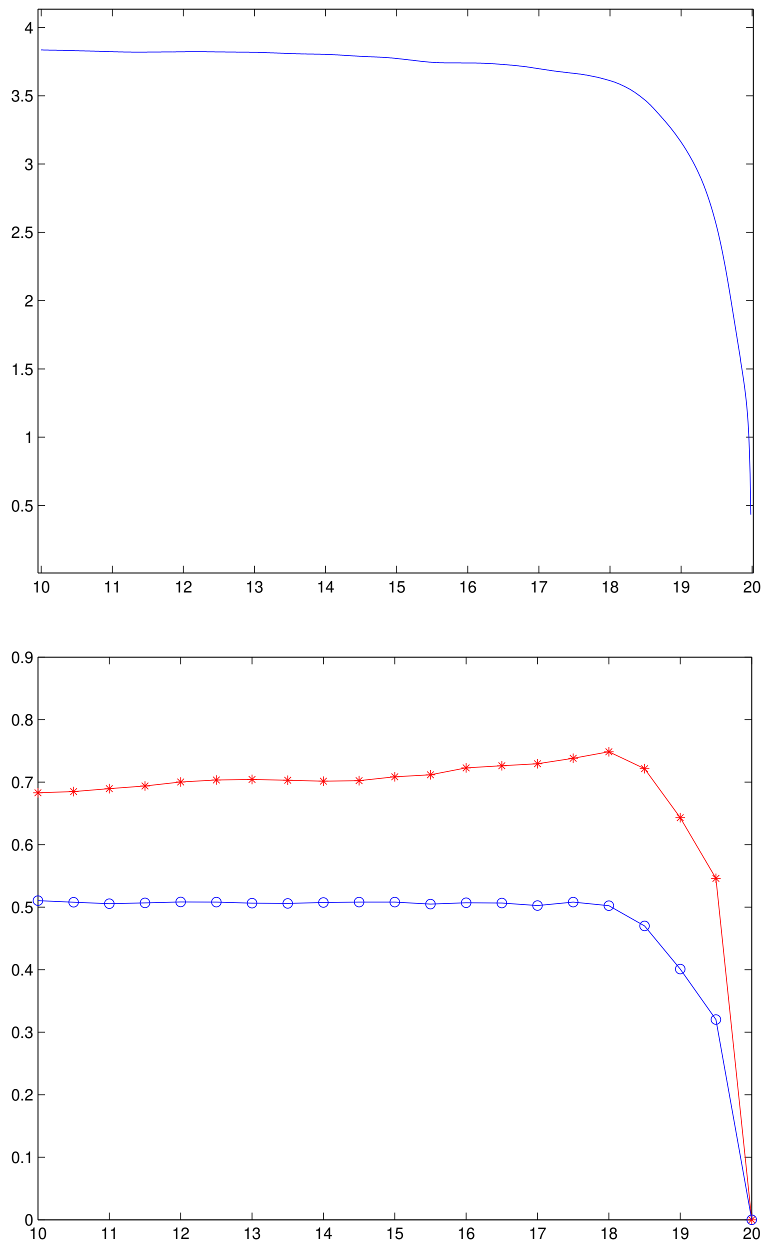

FIGURE 5. Stability factor $S_{1,1}(T_0)$ (upper), and discretization error e_D ($'o'$) and modeling error e_M ($'*'$) (lower), after 13 adaptive mesh refinements as functions of the length of the time interval $[T_0, T]$, with T fix and T_0 varying, assuming $U_h(T_0) = u^h(T_0)$.

residual $R_4(u, U_h)$ is large on the top and the bottom of the channel and in the recirculation zone downstream the cube. The dual velocity, indicating domain of influence for $R_1(U_h, P_h)$ and $R_4(u, U_h)$, is large upstream the cube, along the boundary of the cube, and

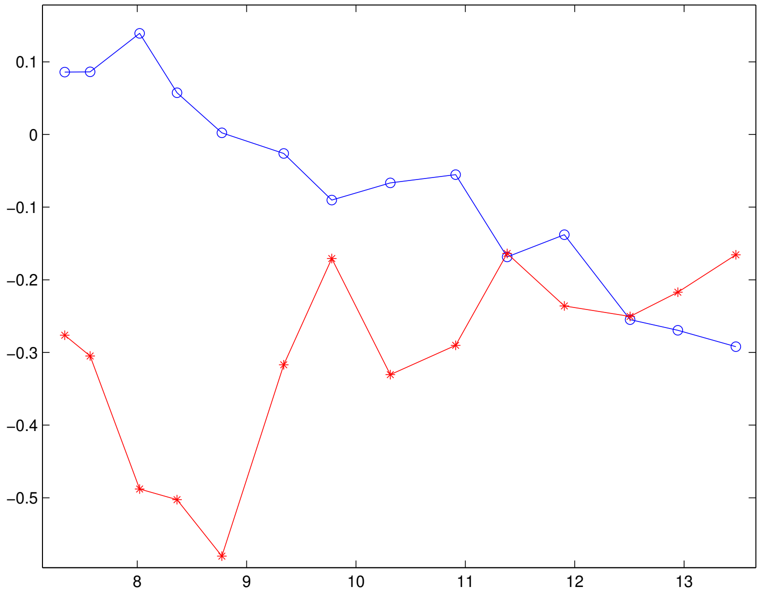

FIGURE 6. A posteriori error estimates of the discretization error e_D $('o')$ and the modeling error e_M $('*')$ for the time interval $[10, 20]$, as functions of the number of degrees of freedom in a log_{10}-log_{10} plot.

in the recirculation zone downstream the cube, and the dual pressure, indicating domain of influence for $R_2(U_h)$, is large near the inlet as well as near the upstream corners of the cube.

In Figure 4 we plot the corresponding drag coefficient as a function of time, and the mean drag coefficient over the time interval $[10, 20]$ as a function of the number of degrees of freedom. We find that even though we do not reach full convergence using the avaliable number of degrees of freedom, the value for the mean drag coefficient seems to asymptotically approach a value between 1.45-1.5.

We know of no experimental reference values of $\bar{c}_D$, but in [28] $\bar{c}_D$ is approximated computationally. The computational setup is similar to the one in this paper except the numerical method, a different length of the time interval, and that we in this paper use a channel of length $15H$, compared to a channel of length $10H$ in [28]. Using different meshes and subgrid models, approximations of $\bar{c}_D$ in the interval $[1.14, 1.24]$ are presented in [28].

After 13 adaptive mesh refinements we have $\sim 1.3 \cdot 10^6$ degrees of freedom, using about 1.5 GB of memory on a regular PC. For $H = 0.1$, the diameter of the smallest element in the mesh $\mathcal{T}_n^{14}$ is about 10^{-3}, which corresponds to a local Reynolds number $Re_{loc} \approx (2H/h)^{4/3} \approx 1200$ (with channel height $2H$), using standard Kolmogorov arguments of turbulent flow [12], or $Re_{loc} \approx h^{-1} = 1000$, assuming the numerical viscosity of the cG(1)cG(1) method is acting as a term $\delta_1(\nabla U_h, \nabla U_h)$ with $\delta_1 \sim h$. That is, we are locally able to resolve scales corresponding to a Reynolds number of about 1000, even though it would be impossible to do globally to a similar computational cost. Since turbulence often is a local phenomena, adaptive methods are ideal for computation of turbulence. In theory, if we refine the same elements in each step of the algorithm we would get a finest $h \approx H \times (1/2)^{13} \approx 10^{-5}$, corresponding to $Re_{loc} \approx 10^5$. *That is, we would be able to locally resolve flows corresponding to a Reynolds number of* 10^5 *in a Direct Numerical Simulation using an ordinary PC or laptop computer.*

4.3. **A posteriori error estimates.** After 13 adaptive mesh refinements we plot the a posteriori error estimates of the discretization and the modeling errors in Figure 5 as functions of the length of the time interval $[T_0, T]$ (T fix, T_0 varying), where we have assumed that the initial solution is exact for each T_0, so that $U_h(T_0) = u^h(T_0)$. We note the similarity to the plot of the stability factor $S_{1,1}(T_0)$, and we find that the error estimates give rather large bounds for the error in the case of longer time averages.

In Figure 6 we plot the discretization and the modeling errors for $\bar{c}_D$ over the time interval $[10, 20]$ as functions of the number of degrees of freedom, where we note an expected decrease in the estimate of the discretization error as we refine the mesh. We also note that the estimate of the modeling error on the other hand increases. This might at first seem alarming, but is in fact to be expected since in this case we have used the simple model (4.1) to estimate the Reynolds stresses in the modeling residual. Even though the true Reynolds stresses are smaller for a finer resolution h of the problem, the model (4.1) will in fact first increase as we resolve more scales of motion since it is solely based on the resolved velocity fluctuations on the scale $2h$, and since we are not using any subgrid model in the computations the estimate of the modeling residual will also increase. This is of course a problem, and in a continuation of this study we seek sharper estimates of the Reynolds stresses based on scale extrapolation.

Remark 7. *The use of a stabilized Galerkin finite element method in the computations may be viewed as a type of subgrid model in itself, since we then in fact solve a modified set of equations using a standard Galerkin method. We will further investigate this relation between numerical stabilization and subgrid modeling in a continuation of this work. In this paper we only consider the stabilization to be part of the numerical method and not an explicit subgrid model. This means in particular that in fact the modeling residual may be overestimated since we do not subtract the contribution from this implicit subgrid model.*

Remark 8. *In each step of Algorithm 2 we mark* $\sim 50\%$ *of the elements for refinement. To get a consistent mesh we have to refine additional elements, so the exact fraction of the elements that are refined each step vary. For more details on mesh refinement algorithms we refer to* [5]*, and the references therin.*

Remark 9. *We have assumed* $R_3(U, P)$ *to be neglible compared to the other residuals in the computations, due to the multiplication by* ν*.*

Remark 10. *In the computations we use a slightly different form of the dual problem (3.3), obtained by partial integration in the term* $((u^h \cdot \nabla)v, \varphi)$*, giving instead* $-((u^h \cdot \nabla)\varphi, v)$*. For pure Dirichlet boundary conditions the two forms are equivalent, but in the case of Neumann boundary conditions the difference is a surface integral of* $(u\varphi) \cdot n$ *multiplied by*

v over the Neumann part of the boundary. In the computations we have a Neumann type outflow boundary condition, but we find that φ is close to zero on this outflow boundary, see Figure 3, and we thus consider our computational approximation of the dual problem to be justified.

Remark 11. *We have used $C^k_{n,K} = 1/2$ and $C^h_{n,K} = 1/8$ as constant approximations of the interpolation constants in Theorem 5. These values are motivated by simple analysis on reference elements.*

5. Summary

In this paper we have proved a posteriori error estimates, and used a corresponding adaptive finite element method to compute approximations of the temporal mean of the drag coefficient in a turbulent flow around a surface mounted cube. The a posteriori error estimates, based on the solution of an associated linearized dual problem, are used to estimate the computational cost associated with the approximation of the mean drag coefficient and as error indicators for the adaptive mesh refinement algorithm.

We emphasize the local nature of turbulence in this problem that makes adaptive methods ideal for efficient and accurate computations. Due to the computational goal of approximating the mean drag coefficient we refine the mesh according to the corresponding a posteriori error estimate, resolving scales of motion corresponding to local Reynolds numbers of about 1000, and in theory we would be able to resolve local scales of motion corresponding to local Reynolds numbers of the order 10^5 to a similar computational cost.

In continuations of this study we will address methods for sharp estimation of the modeling residual, as well as adaptive strategies to combine numerical stabilization with subgrid modeling for LES.

References

[1] R. A. Adams, *Sobolev Spaces*, Academic Press, 1975.

[2] I. Babuška and A. D. Miller, *The post-processing approach in the finite element method, iii: A posteriori error estimation and adaptive mesh selection*, Int. J. Numer. Meth. Eng., 20 (1984), pp. 2311–2324.

[3] R. Becker and R. Rannacher, *A feed-back approach to error control in adaptive finite element methods: Basic analysis and examples*, East-West J. Numer. Math., 4 (1996), pp. 237–264.

[4] ———, *A posteriori error estimation in finite element methods*, Acta Numerica, 10 (2001), pp. 1–103.

[5] J. Bey, *Tetrahedral grid refinement*, Computing, 55 (1995), pp. 355–378.

[6] M. Braack and A. Ern, *A posteriori control of modeling errors and discretization errors*, SIAM J. Multiscale Modeling and Simulation, (2003).

[7] A. Dunca, V. John, and W. J. Layton, *The commutation error of the space averaged navier-stokes equations on a bounded domain*, Journal of Mathematical Fluid Mechanics, (2003).

[8] K. Eriksson, D. Estep, P. Hansbo, and C. Johnson, *Introduction to adaptive method for differential equations*, Acta Numerica, 4 (1995), pp. 105–158.

[9] ———, *Computational Differential Equations*, Studentlitteratur/Cambridge University Press Lund/New York, 1996.

[10] K. Eriksson and C. Johnson, *An adaptive finite element method for linear elliptic problems*, Math. Comp., 50 (1988), pp. 361–383.

[11] L. C. Evans, *Partial Differential Equations*, American Mathematical Society, 1998.
[12] C. Foias, O. Manley, R. Rosa, and R. Temam, *Navier-Stokes Equations and Turbulence*, Cambridge University Press, 2001.
[13] T. Gatski, M. Y. Hussaini, and J. Lumley, *Simulation and Modeling of Turbulent Flow*, Oxford University Press, 1996.
[14] M. Giles, M. Larson, M. Levenstam, and E. Süli, *Adaptive error control for finite element approximations of the lift and drag coefficients in viscous flow*, Technical Report NA-76/06, Oxford University Computing Laboratory, (1997).
[15] J. Hoffman, *On dynamic computational subgrid modeling*, Numerical Analysis Group Preprint, Oxford University, (1999).
[16] ——, *Dynamic Subgrid Modeling for Scalar Convection-Diffusion-Reaction Equations with Fractal Coefficients*, Multiscale and Multiresolution Methods: Theory and Application (Ed. T. J. Barth, T. Chan and R. Haimes), Lecture Notes in Computational Science and Engineering, Springer-Verlag Publishing, Heidelberg, 2001.
[17] ——, *Dynamic subgrid modeling for time dependent convection-diffusion-reaction equations with fractal solutions*, International Journal for Numerical Methods in Fluids, Vol 40, (2001), pp. 583–592.
[18] ——, *Adaptive finite element methods for les: Duality based a posteriori error estimation in various norms and linear functionals*, submitted to SIAM Journal of Scientific Computing, (2002).
[19] ——, *Computation of functionals in 3d incompressible flow for stationary benchmark problems using adaptive finite element methods*, submitted to Mathematical Models and Methods in Applied Sciences (M3AS), (2003).
[20] ——, *Subgrid modeling for convection-diffusion-reaction in 2 space dimensions using a haar multiresolution analysis*, to appear in Mathematical Models and Methods in Applied Sciences, (2003).
[21] J. Hoffman and C. Johnson, *Adaptive finite element methods for incompressible fluid flow*, Error Estimation and Solution Adaptive Discretization in Computational Fluid Dynamics (Ed. T. J. Barth and H. Deconinck), Lecture Notes in Computational Science and Engineering, Springer-Verlag Publishing, Heidelberg, 2002.
[22] J. Hoffman, C. Johnson, and S. Bertoluzza, *Subgrid modeling for convection-diffusion-reaction in 1 space dimension using a haar multiresolution analysis*, to appear in Computer Methods in Applied Mechanics and Engineering, (2003).
[23] P. Houston, R. Rannacher, and E. Süli, *A posteriori error analysis for stabilized finite element approximations of transport problems*, Comput. Mech. Appl. Mech. Engrg., 190 (2000), pp. 1483–1508.
[24] V. John, W. J. Layton, and N. Sahin, *Derivation and analysis of near wall models for channel and recirculating flows*, Preprint 14/02, Fakultät für Mathematik, Otto-von-Guericke-Universität Magdeburg, (2002).
[25] C. Johnson, *Adaptive Finite Element Methods for Conservation Laws*, Advanced Numerical Approximation of Nonlinear Hyperbolic Equations, Springer Lecture Notes in Mathematics, Springer Verlag, 1998.
[26] C. Johnson and R. Rannacher, *On error control in CFD*, Int. Workshop Numerical Methods for the Navier-Stokes Equations (F.K. Hebeker et.al. eds.), Vol. 47 of *Notes Numer. Fluid Mech.*, Vierweg, Braunschweig, 1994, pp. 133–144.
[27] C. Johnson, R. Rannacher, and M. Boman, *Numerics and hydrodynamic stability: Toward error control in cfd*, SIAM J. Numer. Anal., 32 (1995), pp. 1058–1079.
[28] S. Krajnović and L. Davidson, *Large-eddy simulation of the flow around a bluff body*, AIAA Journal, 40 (2002), pp. 927–936.
[29] S. Liu, C. Meneveau, and J. Katz, *On the properties of similarity subgrid-scale models as deduced from measurements in turbulent jet*, J. Fluid Mech., 275 (1994), pp. 83–119.
[30] R. Martinuzzi and C. Tropea, *Flow around a surface mounted cube*, in selected papers of the 1992 Annual Conference on LDA Applications, Lisbon, 1993.

[31] ———, *The flow around a surface mounted, prismatic obstacles placed in a fully developed channel flow*, Trans. ASME, J. Fluids Eng., 115(85) (1993).

[32] U. Piomelli and E. Balaras, *Wall-layer models for large-eddy simulation*, Annu. Rev. Fluid Mech., 34 (2002), pp. 349–374.

[33] R. Rannacher, *Finite element methods for the incompressible navier stokes equations*, Preprint Intsitute of Applied Mathematics, Univ. of Heidelberg, (1999).

[34] P. Sagaut, *Large Eddy Simulation for Incompressible Flows*, Springer-Verlag, Berlin, Heidelberg, New York, 2001.

[35] O. V. Vasilyev, T. S. Lund, and P. Moin, *A general class of commutative filters for les in complex geometries*, Journal of Computational Physics, 146 (1998), pp. 82–104.

Chalmers Finite Element Center Preprints

2001–01 *A simple nonconforming bilinear element for the elasticity problem*
Peter Hansbo and Mats G. Larson

2001–02 *The $\mathcal{LL}^*$ finite element method and multigrid for the magnetostatic problem*
Rickard Bergström, Mats G. Larson, and Klas Samuelsson

2001–03 *The Fokker-Planck operator as an asymptotic limit in anisotropic media*
Mohammad Asadzadeh

2001–04 *A posteriori error estimation of functionals in elliptic problems: experiments*
Mats G. Larson and A. Jonas Niklasson

2001–05 *A note on energy conservation for Hamiltonian systems using continuous time finite elements*
Peter Hansbo

2001–06 *Stationary level set method for modelling sharp interfaces in groundwater flow*
Nahidh Sharif and Nils-Erik Wiberg

2001–07 *Integration methods for the calculation of the magnetostatic field due to coils*
Marzia Fontana

2001–08 *Adaptive finite element computation of 3D magnetostatic problems in potential formulation*
Marzia Fontana

2001–09 *Multi-adaptive galerkin methods for ODEs I: theory & algorithms*
Anders Logg

2001–10 *Multi-adaptive galerkin methods for ODEs II: applications*
Anders Logg

2001–11 *Energy norm a posteriori error estimation for discontinuous Galerkin methods*
Roland Becker, Peter Hansbo, and Mats G. Larson

2001–12 *Analysis of a family of discontinuous Galerkin methods for elliptic problems: the one dimensional case*
Mats G. Larson and A. Jonas Niklasson

2001–13 *Analysis of a nonsymmetric discontinuous Galerkin method for elliptic problems: stability and energy error estimates*
Mats G. Larson and A. Jonas Niklasson

2001–14 *A hybrid method for the wave equation*
Larisa Beilina, Klas Samuelsson and Krister Åhlander

2001–15 *A finite element method for domain decomposition with non-matching grids*
Roland Becker, Peter Hansbo and Rolf Stenberg

2001–16 *Application of stable FEM-FDTD hybrid to scattering problems*
Thomas Rylander and Anders Bondeson

2001–17 *Eddy current computations using adaptive grids and edge elements*
Y. Q. Liu, A. Bondeson, R. Bergström, C. Johnson, M. G. Larson, and K. Samuelsson

2001–18 *Adaptive finite element methods for incompressible fluid flow*
Johan Hoffman and Claes Johnson

2001–19 *Dynamic subgrid modeling for time dependent convection–diffusion–reaction equations with fractal solutions*
Johan Hoffman

2001–20 *Topics in adaptive computational methods for differential equations*
Claes Johnson, Johan Hoffman and Anders Logg

2001–21 *An unfitted finite element method for elliptic interface problems*
Anita Hansbo and Peter Hansbo

2001–22 *A P^2–continuous, P^1–discontinuous finite element method for the Mindlin-Reissner plate model*
Peter Hansbo and Mats G. Larson

2002–01 *Approximation of time derivatives for parabolic equations in Banach space: constant time steps*
Yubin Yan

2002–02 *Approximation of time derivatives for parabolic equations in Banach space: variable time steps*
Yubin Yan

2002–03 *Stability of explicit-implicit hybrid time-stepping schemes for Maxwell's equations*
Thomas Rylander and Anders Bondeson

2002–04 *A computational study of transition to turbulence in shear flow*
Johan Hoffman and Claes Johnson

2002–05 *Adaptive hybrid FEM/FDM methods for inverse scattering problems*
Larisa Beilina

2002–06 *DOLFIN - Dynamic Object oriented Library for FINite element computation*
Johan Hoffman and Anders Logg

2002–07 *Explicit time-stepping for stiff ODEs*
Kenneth Eriksson, Claes Johnson and Anders Logg

2002–08 *Adaptive finite element methods for turbulent flow*
Johan Hoffman

2002–09 *Adaptive multiscale computational modeling of complex incompressible fluid flow*
Johan Hoffman and Claes Johnson

2002–10 *Least-squares finite element methods with applications in electromagnetics*
Rickard Bergström

2002–11 *Discontinuous/continuous least-squares finite element methods for elliptic problems*
Rickard Bergström and Mats G. Larson

2002–12 *Discontinuous least-squares finite element methods for the Div-Curl problem*
Rickard Bergström and Mats G. Larson

2002–13 *Object oriented implementation of a general finite element code*
Rickard Bergström

2002–14 *On adaptive strategies and error control in fracture mechanics*
Per Heintz and Klas Samuelsson

2002–15 *A unified stabilized method for Stokes' and Darcy's equations*
Erik Burman and Peter Hansbo

2002–16 *A finite element method on composite grids based on Nitsche's method*
Anita Hansbo, Peter Hansbo and Mats G. Larson

2002–17 *Edge stabilization for Galerkin approximations of convection–diffusion problems*
Erik Burman and Peter Hansbo

2002–18	*Adaptive strategies and error control for computing material forces in fracture mechanics* Per Heintz, Fredrik Larsson, Peter Hansbo and Kenneth Runesson
2002–19	*A variable diffusion method for mesh smoothing* J. Hermansson and P. Hansbo
2003–01	*A hybrid method for elastic waves* L.Beilina
2003–02	*Application of the local nonobtuse tetrahedral refinement techniques near Fichera-like corners* L.Beilina, S.Korotov and M. Křížek
2003–03	*Nitsche's method for coupling non-matching meshes in fluid-structure vibration problems* Peter Hansbo and Joakim Hermansson
2003–04	*Crouzeix–Raviart and Raviart–Thomas elements for acoustic fluid–structure interaction* Joakim Hermansson
2003–05	*Smoothing properties and approximation of time derivatives in multistep backward difference methods for linear parabolic equations* Yubin Yan
2003–06	*Postprocessing the finite element method for semilinear parabolic problems* Yubin Yan
2003–07	*The finite element method for a linear stochastic parabolic partial differential equation driven by additive noise* Yubin Yan
2003–08	*A finite element method for a nonlinear stochastic parabolic equation* Yubin Yan
2003–09	*A finite element method for the simulation of strong and weak discontinuities in elasticity* Anita Hansbo and Peter Hansbo
2003–10	*Generalized Green's functions and the effective domain of influence* Donald Estep, Michael Holst, and Mats G. Larson
2003–11	*Adaptive finite element/difference method for inverse elastic scattering waves* L.Beilina
2003–12	*A Lagrange multiplier method for the finite element solution of elliptic domain decomposition problems using non-matching meshes* Peter Hansbo, Carlo Lovadina, Ilaria Perugia, and Giancarlo Sangalli
2003–13	*A reduced P^1–discontinuous Galerkin method* R. Becker, E. Burman, P. Hansbo, and M. G. Larson
2003–14	*Nitsche's method combined with space–time finite elements for ALE fluid–structure interaction problems* Peter Hansbo, Joakim Hermansson, and Thomas Svedberg
2003–15	*Stabilized Crouzeix–Raviart element for the Darcy-Stokes problem* Erik Burman and Peter Hansbo
2003–16	*Edge stabilization for the generalized Stokes problem: a continuous interior penalty method* Erik Burman and Peter Hansbo

2003–17 *A conservative flux for the continuous Galerkin method based on discontinuous enrichment*
Mats G. Larson and A. Jonas Niklasson

2003–18 *CAD–to–CAE integration through automated model simplification and adaptive modelling*
K.Y. Lee, M.A. Price, C.G. Armstrong, M.G. Larson, and K. Samuelsson

2003–19 *Multi-adaptive time integration*
Anders Logg

2003–20 *Adaptive computational methods for parabolic problems*
Kenneth Eriksson, Claes Johnson, and Anders Logg

2003–21 *The FEniCS project*
T. Dupont, J. Hoffman, C. Johnson, R. Kirby, M. Larson, A. Logg, and R. Scott

2003–22 *Adaptive finite element methods for LES: Computation of the mean drag coefficient in a turbulent flow around a surface mounted cube using adaptive mesh refinement*
Johan Hoffman

These preprints can be obtained from

www.phi.chalmers.se/preprints